

Heat transport through quantum Rabi model

Tsuyoshi Yamamoto* and Takeo Kato

Institute for Solid State Physics, the University of Tokyo, Kashiwa, Chiba 277-8581, Japan

(Dated: April 2, 2022)

We investigate heat transport through quantum Rabi model, which is composed of a two-state system and two harmonic oscillators, as a prototype of heat devices using controllable multi-level systems. Using the noninteracting-blip approximation (NIBA), we find that the linear thermal conductance shows a characteristic temperature dependence with a two-peak structure. We also show that heat transport is sensitive to model parameters for weak system-bath coupling and strong hybridization between the two-state system and the harmonic oscillators. This property characteristic of the multi-level system is advantageous for applications such as a heat transistor, and can be examined in superconducting circuits.

I. INTRODUCTION

Heat transport through nanoscale objects has attracted interest for a long period of time from the viewpoint of both fundamental physics on quantum mechanics [1–4] and application to heat devices [5]. Various heat devices (e.g., heat rectification [6, 7], heat transistor [8, 9], quantum refrigerator [10], and quantum heat engine [11]) have been theoretically proposed as analogy to electronic nanoscale devices. Recently, some of them have been implemented in various physical systems using nanostructures [12–14].

Recent advances in circuit quantum electrodynamics (QED) using superconductor devices [15–17] have led to considerable developments in the study of heat transport through small quantum objects. The circuit QED system provides an ideal platform for the study of heat transport [12, 13], in which superconducting qubits [18–20] can be coupled to quantum resonators or transmission lines with well-controlled coupling strengths. In fact, heat transport in superconducting circuits has been measured with high accuracy in recent experiments [21–23].

In the theoretical studies on heat transport, the spin-boson model [24, 25] has been widely used as a simple prototype system [6, 26–32]. However, this model is too simple for the discussion of sophisticated control of heat devices, because the number of independent model parameters is not large. As a model with more parameters, the two-level system embedded between two harmonic oscillators can be considered (see Fig. 1), which is an archetype of small systems with multiple levels described by the quantum Rabi model [33]. Although the quantum Rabi model is still simple and fundamental, it has sufficient flexibility for designing multiple quantum levels of the system. We should note that heat transport of this setup has indeed been measured in recent experiments using a superconducting circuit [12, 13]. However, these implementations are restricted to weak hybridization between the two-state and the harmonic oscillators, and the regime of the ultra-strong hybridization has not

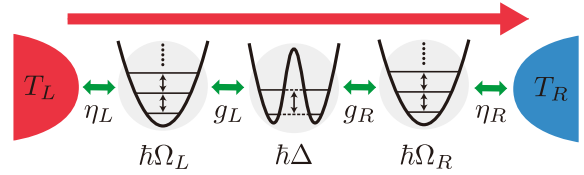


FIG. 1. Schematic of heat transport through a small system described by the quantum Rabi model, in which a two-state system with a tunneling splitting frequency Δ is embedded between two harmonic oscillators with a natural frequency Ω_r ($r = L, R$). When the temperature of the left heat bath is larger than that of the right one ($T_L > T_R$), heat flow is induced through the quantum Rabi model from the left to the right. In this study, we consider the case of $\Omega_L = \Omega_R \equiv \Omega$ and $\eta_L = \eta_R \equiv \eta$.

been studied yet experimentally and theoretically.

In this work, we explore heat transport through the quantum Rabi model between the Ohmic heat baths whose spectral density function is linear to the frequency. We reveal several features of heat transport through the quantum Rabi model, that cannot be observed in simple systems such as the spin-boson model. We find that the thermal conductance has a two-peak structure as a function of the temperature when the harmonic oscillators are strongly hybridized with the two-state system under weak system-bath coupling. In this situation, heat transport becomes sensitive to the parameters (e.g., the natural frequency of the harmonic oscillators and the tunneling splitting of the two-state system), and a certain value of the parameter induces the enhancement of the heat flux. We clarify the origin of this sensitivity, which is advantageous to applications of heat devices, from the energy spectrum of the quantum Rabi model.

The rest of this paper is organized as follows. In Sec. II, we introduce the dissipative quantum Rabi model and derive the formula for the linear thermal conductance. We also present limiting cases, which allow analytic calculation. In Sec. III, we introduce a non-perturbative approximation, the noninteracting-blip approximation (NIBA) [24, 25], and obtain an approximate expression for the linear thermal conductance. In Sec. IV,

* t.yamamoto@issp.u-tokyo.ac.jp

we discuss how the thermal conductance depends on the temperature and the natural frequency of the harmonic oscillators. Finally, we summarize our work in Sec. V.

II. FORMULATION

In this section, we introduce a model that describes the setup in Fig. 1 and formulate a thermal conductance by using the Keldysh formalism, providing the Meir-Wingreen-Landauer-type heat current [27]. In addition, we briefly summarize the weak-coupling theory and renormalization effect due to the system-reservoir coupling.

A. Model

We consider heat transport through a quantum Rabi model, whose Hamiltonian is given as

$$H_q = -\frac{\hbar\Delta}{2}\sigma_x + \sum_r \hbar\Omega_r a_r^\dagger a_r + \sum_r \hbar g_r \sigma_z (a_r + a_r^\dagger), \quad (1)$$

where a_r (a_r^\dagger) is an annihilation (a creation) operator of the harmonic oscillator r ($= L, R$), $\sigma_{x,y,z}$ are Pauli matrices, Δ is a tunneling splitting frequency [34], Ω_r is a natural frequency of the harmonic oscillator r , and the frequency g_r represents the coupling strength between the two-state system and the harmonic oscillator r (see Fig. 1).

The two heat baths are modeled as a collection of harmonic oscillators. The Hamiltonian of the heat bath r ($= L, R$) is given as

$$H_r = \sum_k \hbar\omega_{r,k} b_{r,k}^\dagger b_{r,k} \quad (2)$$

with an annihilation (a creation) operator $b_{r,k}$ ($b_{r,k}^\dagger$) of the k -th bosonic mode with the frequency $\omega_{r,k}$ in the heat bath r . The total Hamiltonian is given as

$$H = H_q + \sum_r (H_r + H_{\text{int},r}), \quad (3)$$

where $H_{\text{int},r}$ describes the coupling between the harmonic oscillator r and the heat bath r :

$$H_{\text{int},r} = \sum_k \hbar\lambda_{r,k} (a_r + a_r^\dagger) (b_{r,k} + b_{r,k}^\dagger). \quad (4)$$

Here, the frequency $\lambda_{r,k}$ represents the coupling strength between the harmonic oscillator r and the k -th bosonic mode in the heat bath r . Each of the heat baths is completely characterized by a spectral density

$$I_r(\omega) = \sum_k \lambda_{r,k}^2 \delta(\omega - \omega_{r,k}). \quad (5)$$

We assume that the number of bosonic modes is so large that the spectral density $I_r(\omega)$ can be considered as a smooth function of the frequency. We consider the Ohmic baths, for which the spectral density is linear with respect to ω :

$$I_r(\omega) = 2\eta_r\omega. \quad (6)$$

Here, η_r represents a dimensionless coupling strength between the heat bath r and the harmonic oscillator r . For simplicity, we consider the symmetric case, $\Omega_L = \Omega_R \equiv \Omega$ and $\eta_L = \eta_R \equiv \eta$.

B. Mapping to the effective spin-boson model

By diagonalizing the combined system composed of the heat baths and the harmonic oscillators, the dissipative quantum Rabi model (3) can be mapped to the spin-boson model [35–38]

$$H_{\text{SB}} = -\frac{\hbar\Delta}{2}\sigma_x + \sum_{r,k} \hbar\omega_{r,k} b_{r,k}^\dagger b_{r,k} - \frac{\sigma_z}{2} \sum_{r,k} \hbar\tilde{\lambda}_{r,k} (b_{r,k} + b_{r,k}^\dagger), \quad (7)$$

with an effective spectral density, which is called as the structured spectral density,

$$I_{\text{eff},r}(\omega) = \sum_k \tilde{\lambda}_{r,k}^2 \delta(\omega - \omega_{r,k}) = \alpha_r \tilde{I}_{\text{eff}}(\omega), \quad (8)$$

$$\tilde{I}_{\text{eff}}(\omega) = 2\omega \frac{\Omega^4}{(\Omega^2 - \omega^2)^2 + (2\Gamma\omega)^2}. \quad (9)$$

Here, the two harmonic oscillators are incorporated into the effective Lorentz-type spectral density, which is characterized by the peak frequency Ω , the peak width $\Gamma = \pi\eta\Omega$, and the dimensionless coupling strength $\alpha_r = \eta(4g_r/\Omega)^2$.

C. Thermal conductance

The heat current from the heat bath r into the system described by the quantum Rabi model (1) is defined as

$$J_r \equiv -\frac{dH_r}{dt}. \quad (10)$$

For the effective spin-boson model (7), the steady-state heat current is calculated by the Keldysh formalism as [8, 39, 40]

$$\langle J \rangle = \frac{\alpha\gamma\hbar^2}{8} \int_0^\infty d\omega \omega \tilde{I}_{\text{eff}}(\omega) \text{Im}[\chi(\omega)] [n_L(\omega) - n_R(\omega)], \quad (11)$$

where $\alpha = \alpha_L + \alpha_R$, $\gamma = 4\alpha_L\alpha_R/\alpha^2$, $n_r(\omega) = (e^{\beta_r\hbar\omega} - 1)^{-1}$ is the Bose-Einstein distribution function for the

heat bath r , $\beta_r = (k_B T_r)^{-1}$, k_B is the Boltzmann constant, T_r is the temperature of the heat bath r , and $\chi(\omega)$ is the dynamic susceptibility of the two-state system defined as

$$\chi(\omega) = -\frac{i}{\hbar} \int_0^\infty dt e^{i\omega t} \langle [\sigma_z(t), \sigma_z(0)] \rangle. \quad (12)$$

The liner thermal conductance is given as

$$\begin{aligned} \kappa &\equiv \lim_{\Delta T \rightarrow 0} \frac{\langle J \rangle}{\Delta T} \\ &= \frac{\alpha\gamma\hbar k_B}{8} \int_0^\infty d\omega \tilde{I}_{\text{eff}}(\omega) \text{Im}[\chi(\omega)] \left[\frac{\beta\hbar\omega/2}{\sinh(\beta\hbar\omega/2)} \right]^2, \end{aligned} \quad (13)$$

with $\Delta T = T_L - T_R$. For the convenience of analysis, we introduce a symmetrized correlation function,

$$S(t) = \frac{1}{2} \langle \sigma_z(t)\sigma_z(0) + \sigma_z(0)\sigma_z(t) \rangle. \quad (14)$$

By the fluctuation-dissipation theorem [25], the imaginary part of the dynamic susceptibility is related to the Fourier transformation of $S(t)$ as

$$S(\omega) = \hbar \coth \left(\frac{\beta\hbar\omega}{2} \right) \text{Im}[\chi(\omega)]. \quad (15)$$

Then, the liner thermal conductance is then rewritten with $S(\omega)$ as

$$\kappa = \frac{\alpha\gamma k_B}{16} \int_0^\infty d\omega \tilde{I}_{\text{eff}}(\omega) S(\omega) \frac{(\beta\hbar\omega)^2}{\sinh(\beta\hbar\omega)}. \quad (16)$$

Due to the factor $(\beta\hbar\omega)^2/\sinh(\beta\hbar\omega)$, the thermal conductance is mainly determined by the behavior of $S(\omega)$ in the region of $0 < \omega \lesssim k_B T/\hbar$.

D. Renormalized Ohmic spin-boson model derived for $\Delta \ll \Omega$

For $\Delta \ll \Omega$, the effective spectral density (9) can be regarded as a two-state system coupled to the Ohmic bath with a dimensionless system-bath coupling strength $\alpha_r = \eta(4g_r/\Omega)^2$ and a high-frequency cutoff $\Omega (\gg \Delta)$. Then, heat transport in this regime can be understood by simply referring the results on heat transport via a two-state system [6, 26, 27, 31, 41]. This parameter regime is not preferable to control heat transport because this effective two-state system shows a rather simple behavior for heat transport with respect to the parameters. In fact, the parameters regarding the harmonic oscillators, i.e., Ω_r , g_r , and η , are absorbed into a single parameter Δ_* , which is the renormalized tunneling splitting frequency obtained by the adiabatic renormalization [24]. In this study, we focus on the opposite regime, i.e., the case of $\Delta \gtrsim \Omega$, in which the present model exhibits non-trivial transport properties.

E. Weak-coupling regime ($\eta \ll 1$)

It is helpful to consider the weak-coupling regime ($\eta \ll 1$). For the isolated quantum Rabi model ($\eta = 0$), we denote the eigen energy and the corresponding eigen state as $\hbar\omega_n$ and $|n\rangle$, respectively:

$$H_q |n\rangle = \hbar\omega_n |n\rangle, \quad (n = 0, 1, 2, \dots). \quad (17)$$

Then, the symmetrized correlation function $S(\omega)$ is described as

$$\begin{aligned} S(\omega) &= \frac{\pi}{Z_q} \sum_{n,m} e^{-\beta\hbar\omega_m} |\langle n|\sigma_z|m \rangle|^2 \\ &\quad \times [\delta(\omega - \omega_{nm}) + \delta(\omega + \omega_{nm})], \end{aligned} \quad (18)$$

where $Z_q = \text{tr}[e^{-\beta H_q}]$ and $\omega_{nm} = \omega_n - \omega_m$ is the transition frequency. When switching on the system-bath coupling η , the delta function peaks in $S(\omega)$ are replaced by those with finite widths. In general, their positions and widths vary when η increases from zero. However, in the weak-coupling regime ($\eta \ll 1$) these effects are so weak that the expression of $S(\omega)$ given in Eq. (18) can be used approximately.

At low temperatures, $S(\omega)$ is determined mainly by transitions from the ground state. Then, the symmetrized correlation function is approximated as

$$S(\omega) \approx \pi \sum_n |\langle n|\sigma_z|0 \rangle|^2 [\delta(\omega - \omega_{n0}) + \delta(\omega + \omega_{n0})]. \quad (19)$$

By substituting this expression into Eq. (16), the thermal conductance is obtained by

$$\kappa \approx \frac{\pi\alpha\gamma k_B}{16} \sum_n |\langle n|\sigma_z|0 \rangle|^2 \tilde{I}_{\text{eff}}(\omega_{n0}) \frac{(\beta\hbar\omega_{n0})^2}{\sinh(\beta\hbar\omega_{n0})}. \quad (20)$$

As a simple example, let us consider the condition $k_B T \sim \hbar\omega_{10}$ and $\omega_{10} \ll \omega_{n0}$ for $n \geq 2$. Then, the thermal conductance is obtained as

$$\kappa \approx \frac{\pi\alpha\gamma k_B}{16} \tilde{I}_{\text{eff}}(\omega_{10}) \frac{(\beta\hbar\omega_{10})^2}{\sinh(\beta\hbar\omega_{10})}. \quad (21)$$

In this example, the thermal conductance shows the Schottky-type temperature dependence [6, 26, 27, 31]; it has a peak at approximately $T \simeq \hbar\omega_{10}/k_B$ and shows exponential suppression ($\kappa \sim T^{-2} e^{-\hbar\omega_{10}/k_B T}$) for $T \ll \hbar\omega_{10}/k_B$.

If the transition energy to the second excited state, $\hbar\omega_{20}$, is also comparable to $k_B T$, the temperature dependence of the thermal conductance is written as a sum of the two Schottky functions. This implies that the thermal conductance may have *two peaks* as a function of the temperature. We will discuss this possibility in Sec. IV in details. The present weak-coupling approximation is useful for qualitative discussion on the temperature dependence of the thermal conductance. However, because the system-bath coupling actually affect the peak position and peak broadening, we need a more sophisticated approximation for quantitative discussion. In the next section, we introduce an alternative approximation.

III. NIBA

In this section, we formulate the thermal conductance using the noninteracting-blip approximation (NIBA), which works well in a wide parameter region including the strong system-bath coupling regime [24, 25, 31]. The time evolution of the population $\langle \sigma_z(t) \rangle$ is generally described by the generalized master equation

$$\frac{d\langle \sigma_z(t) \rangle}{dt} = - \int_0^t dt' K_z(t-t') \langle \sigma_z(t') \rangle, \quad (22)$$

with the kernel $K_z(t)$. In the NIBA, the non-local kernel takes a simple form,

$$K_z(t) = \Delta^2 e^{-Q'(t)} \cos Q''(t), \quad (23)$$

where $Q(t) = Q'(t) + iQ''(t)$ is the complex bath correlation function, whose real and imaginary parts are given as

$$Q'(t) = \int_0^\infty d\omega \frac{I_{\text{eff}}(\omega)}{\omega^2} \coth\left(\frac{\beta\hbar\omega}{2}\right) (1 - \cos\omega t), \quad (24)$$

$$Q''(t) = \int_0^\infty d\omega \frac{I_{\text{eff}}(\omega)}{\omega^2} \sin\omega t, \quad (25)$$

respectively. Using the effective spectral density given in Eqs. (8) and (9), the explicit expressions of $Q'(t)$ and $Q''(t)$ are calculated as [38, 42],

$$Q'(t) = \pi\alpha \left[\frac{2}{\hbar\beta} t - L (e^{-\Gamma t} \cos\bar{\Omega}t - 1) - Ze^{-\Gamma t} \sin\bar{\Omega}t + Q'_{\text{Mats}}(t) \right], \quad (26)$$

$$Q''(t) = \pi\alpha [1 - e^{-\Gamma t} (\cos\bar{\Omega}t - N \sin\bar{\Omega}t)], \quad (27)$$

where

$$\bar{\Omega} = \sqrt{\Omega^2 - \Gamma^2}, \quad (28)$$

$$N = (\Omega^2 - 2\Gamma^2)/(2\Gamma\bar{\Omega}), \quad (29)$$

$$L = \frac{N \sinh(\beta\hbar\bar{\Omega}) - \sin(\beta\hbar\Gamma)}{\cosh(\beta\hbar\bar{\Omega}) - \cos(\beta\hbar\Gamma)}, \quad (30)$$

$$Z = \frac{\sinh(\beta\hbar\bar{\Omega}) + N \sin(\beta\hbar\Gamma)}{\cosh(\beta\hbar\bar{\Omega}) - \cos(\beta\hbar\Gamma)}, \quad (31)$$

and $Q'_{\text{Mats}}(t)$ is a series with respect to the Matsubara frequency $\nu_n = 2\pi n/(\hbar\beta)$ defined as

$$Q'_{\text{Mats}}(t) = \frac{4\Omega^4}{\hbar\beta} \sum_{n=1}^{\infty} \frac{1}{\nu_n} \frac{1 - e^{-\nu_n t}}{(\Omega^2 + \nu_n^2)^2 - (2\Gamma\nu_n)^2}. \quad (32)$$

The symmetrized correlation function $S(\omega)$ can be related to the kernel as [25]

$$S(\omega) = \text{Re} \left[\frac{2}{-i\omega + \hat{K}_z(-i\omega)} \right], \quad (33)$$

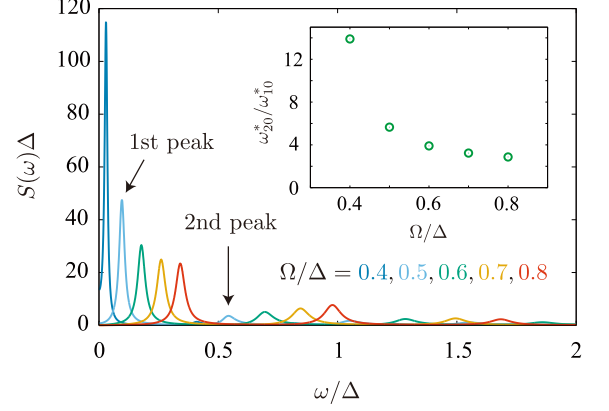


FIG. 2. Symmetrized correlation function $S(\omega)$ as a function of the frequency for different Ω/Δ at fixed other parameters $g = 0.5\Delta$, $\eta = 0.01$, $k_B T = 0.01\hbar\Delta$. $S(\omega)$ has several peaks and the peaks at the lower frequency are more dominant. The arrows indicate the first peak at $\omega_{10}^* = 0.096\Delta$ and the second peak at $\omega_{20}^* = 0.54\Delta$ for $\Omega = 0.5\Delta$. The inset represents a ratio between the frequencies of the first and second peaks, $\omega_{10}^*/\omega_{20}^*$, as a function of Ω/Δ .

where $\hat{K}_z(\lambda)$ is the Laplace transform of $K_z(t)$. By substituting this expression for the symmetrized correlation function into Eq. (16), we can calculate the liner thermal conductance in the NIBA. In general, the NIBA is justified (a) at arbitrary temperatures for the weak system-bath coupling or (b) for incoherent transport realized at the high temperature or the strong system-bath coupling [24, 25]. When the system-bath coupling is not weak, the NIBA fails at low temperatures where heat transport induced by virtual excitations is dominant [31]. However, the deviation from the exact result remains small as far as the system-bath coupling is weak.

IV. RESULT

In this section, we present the results calculated by the NIBA for $\Omega \lesssim \Delta$, where heat transport is expected to be non-trivial, as discussed in Sec II D.

First, we show the symmetrized correlation function $S(\omega)$ in Fig. 2 for $g = 0.5\Delta$, $\eta = 0.01$, and $k_B T = 0.01\hbar\Delta$. As seen in the figure, $S(\omega)$ has several peaks corresponding to the transition frequencies of the quantum Rabi model as indicated by the approximation for the weak-coupling regime (see Sec. II E). However, the peak positions are shifted from the bare transition frequencies due to the system-bath coupling even for $\eta = 0.01$. For later discussion, we define the frequency of the n -th peak in $S(\omega)$ as ω_{n0}^* . We note that ω_{n0}^* can be regarded as the renormalized transition frequency corresponding to the bare transition frequency ω_{n0} .

Next, we show the temperature dependence of the thermal conductance in Fig. 3 (a) for $g = 0.5\Delta$ and $\eta = 0.01$. For $\Omega/\Delta = 0.4$, we observe a clear two-peak

structure in the temperature dependence. We also observe that the two-peak structure becomes less significant when Ω/Δ is varied from 0.4 to 0.8. This feature in the thermal conductance originates from the first and second peaks of $S(\omega)$, whose frequencies are given by ω_{10}^* and ω_{20}^* (see Fig. 2). Then, its temperature dependence is qualitatively described by the sum of the two Schottky-type functions, $T^{-2}e^{-\hbar\omega_{10}^*/k_B T}$ and $T^{-2}e^{-\hbar\omega_{20}^*/k_B T}$, which leads to the double-peak structure.

The two-peak structure is a signature of the multiple levels characteristic of the quantum Rabi model and can be clearly observed only when the symmetrized correlation function has sharp well-separated peaks. We show the temperature dependence of the thermal conductance for $\Omega = 0.5\Delta$ and $g = 0.5\Delta$ in Fig. 3 (b). When η increases from 0.01 to 0.1, the peak at the low-temperature side becomes less significant. This is because the peaks in $S(\omega)$ are broadened due to the system-bath coupling and are smoothed out after performing the integral in Eq. (16).

Let us discuss the detailed condition for the appearance of the two-peak structure in the thermal conductance (16). If the peaks in the symmetrized correlation function $S(\omega)$ are sufficiently sharp, the thermal conductance is approximately evaluated as

$$\kappa(T) \sim a_1 \frac{e^{-1/\tilde{T}}}{(k_B T)^2} + a_2 \frac{e^{-(\omega_{20}^*/\omega_{10}^*)/\tilde{T}}}{(k_B T)^2}, \quad (34)$$

where $\tilde{T} = k_B T / \hbar\omega_{10}^*$, and the prefactors are given as

$$a_n = \frac{\pi\alpha\gamma k_B}{8} |\langle n | \sigma_z | 0 \rangle|^2 (\hbar\omega_{n0})^2 \tilde{I}_{\text{eff}}(\omega_{n0}^*). \quad (35)$$

The two-peak structure in the temperature dependence of the thermal conductance appears when $\omega_{20}^*/\omega_{10}^* \gg 1$ [43]. This condition can be confirmed by the comparison between Figs. 2 and 3 (a). When Ω/Δ increases from 0.4 to 0.8, the ratio between the frequencies of the first and second peaks, $\omega_{20}^*/\omega_{10}^*$, is reduced from 13.9 to 2.87 (see the inset in Fig. 2). According to the reduction of $\omega_{20}^*/\omega_{10}^*$, the two-peak structure becomes less significant when Ω/Δ increases, see Fig. 3 (a). This feature can be also confirmed by the dependence of the hybridization constant g . Fig 3 (c) shows the temperature dependence of the thermal conductance for $\Omega = 0.5\Delta$ and $\eta = 0.01$. It is observed that when g/Δ increases from 0.3 to 0.7, the two-peak structure becomes more significant. This is because the ratio $\omega_{20}^*/\omega_{10}^*$ is enlarged by the level repulsion when the hybridization g increases.

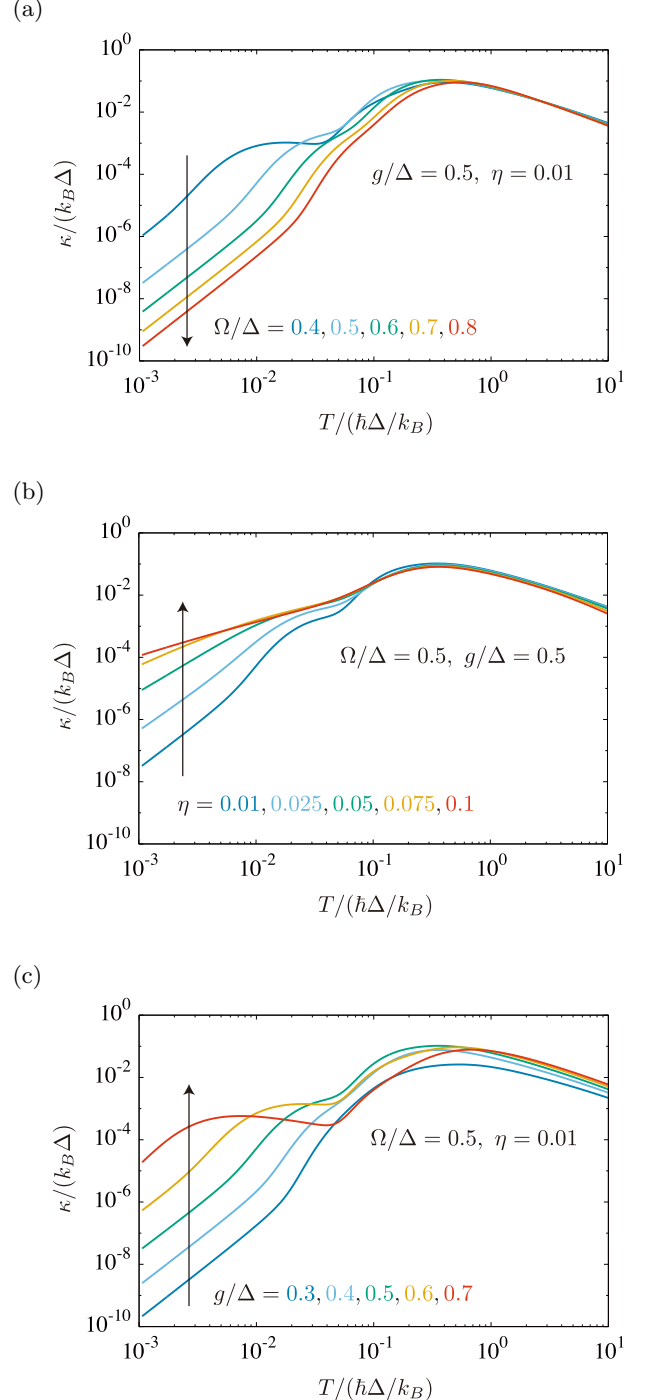


FIG. 3. Temperature dependence of the thermal conductance for typical parameters $\Omega/\Delta = 0.5$, $g/\Delta = 0.5$, and $\eta = 0.01$. When one varies (a) $\Omega/\Delta = 0.4 - 0.8$, (b) $\eta = 0.01 - 0.1$, and (c) $g/\Delta = 0.3 - 0.7$, the thermal conductance considerably changes between the one- and two-peak structures.

When we choose the parameters for which the two-peak structure in $\kappa(T)$ is clearly observed, the thermal conductance is sensitive to the parameters, particularly to Ω/Δ . In Fig. 4, we show the thermal conductance as

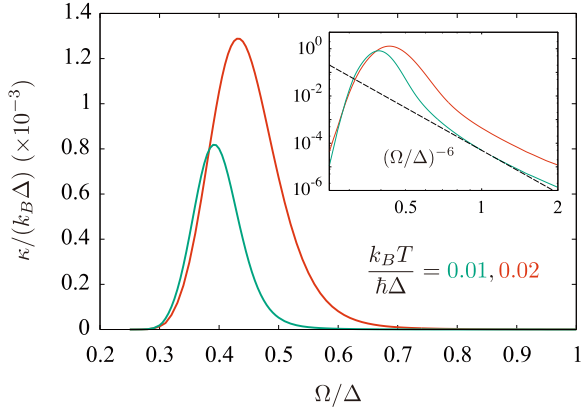


FIG. 4. Thermal conductance as a function of Ω/Δ for $g/\Delta = 0.5$, $\eta = 0.01$, and different temperatures $k_B T = 0.01\hbar\Delta$ and $0.02\hbar\Delta$. The inset is an enlarged view of the high-frequency side of the peak frequency. The dashed line represents a guide for the power law $(\Omega/\Delta)^{-6}$.

a function of Ω/Δ for two different temperatures. The thermal conductance has a sharp peak at $\Omega = \Omega_0$, where $\Omega_0 \approx 0.40\Delta$ and 0.44Δ for $k_B T = 0.01\hbar\Delta$ and $0.02\hbar\Delta$, respectively. The thermal conductance decays exponentially in the small- Ω side of the peak, while it shows a power-law decay in the opposite side, whose exponent is -6 (see the inset in Fig. 4). The strong dependence of Ω/Δ has an advantage for application of heat transistor or heat valves in mesoscopic heat devices.

Finally, we indicate that the power-law decay in $\kappa(\Omega)$ for large Ω/Δ is a signature of the co-tunneling process in which heat transport is induced by the tunneling process via virtual excitations [26, 27, 31]. At low temperatures ($k_B T \ll \hbar\Gamma$, $\hbar\Omega$, $\hbar\omega_{20}^*$), it is supposed the system behaves effectively like the Ohmic spin-boson model with a single parameter ω_{10}^* because the high-energy states are not relevant. Furthermore, for $k_B T \lesssim 0.1\hbar\omega_{10}^*$, thermal excitation from the ground state to the first excited state is strongly suppressed, and heat transport is governed by the co-tunneling process for which the thermal conductance is written as [26, 27, 31]

$$\kappa \approx \frac{\pi^3 \gamma k_B^4}{30} \alpha^2 \chi_0^2 T^3, \quad (36)$$

where χ_0 is the static susceptibility of the effective spin-boson model that is roughly approximated as $2/(\hbar\omega_{10}^*)$ for the weak coupling ($\alpha \ll 1$). Noting that $\alpha = \eta(4g/\Omega)^2$ and $\omega_{10}^* \propto \Omega$ for $\Omega \lesssim \Delta$, we obtain $\kappa(\Omega) \propto \Omega^{-6}$, which is consistent with the numerical result shown in the inset in Fig. 4.

V. CONCLUSION

We studied heat transport through the quantum Rabi model using the non-interacting blip approximation

(NIBA). The thermal conductance shows the two-peak temperature dependence due to the multiple levels in the quantum Rabi model. In addition, we found that the thermal conductance is highly sensitive to the parameters, particularly the natural frequency of the harmonic oscillators in the strong hybridization region $\Omega \sim g \lesssim \Delta$. This property is advantageous to the application of well-controllable heat devices such as a heat transistor.

In general, heat transport through a quantum system with multiple levels may show the same sensitivity to the parameter when its lowest three energy levels are appropriately designed, as done in this work. However, the feature of heat transport obtained in this paper is expected to be well examined in a physical system described by the quantum Rabi model because it is rather feasible to realize it in various physical systems. The dissipative quantum Rabi model can also be regarded as the spin-boson model with the structured spectral density, as mentioned in Sec. II B. Therefore, our result should be applicable to various physical systems (e.g., the chemical reactions in biomolecules [35] and atoms in cavities [44]), which are described by the spin-boson model with the structured spectral density.

The most promising candidate for realizing a system described by the quantum Rabi model is a superconducting circuit, which can be fabricated by the current technology on circuit QED. The quantum Rabi model has been a fundamental model to study the ultra-strong (or deep-strong) coupling between superconducting qubits and resonators [45–48], and its implementation technique accessible to the ultra-strong coupling regime has been developed. By coupling the resonators to superconducting waveguides, which play the role of the Ohmic heat bath, heat transport through the quantum Rabi model can be studied. Indeed, a similar setup has been implemented experimentally using a transmon qubit and superconducting transmission lines, and the heat flow through them has been measured with high accuracy [12], although it does not reach the ultra-strong coupling regime. We hope that the heat transport properties that appear in the ultra-strong coupling regime discussed in this work will be observed experimentally in the near future.

ACKNOWLEDGEMENT

This work was supported by Grant-in-Aid for JSPS Fellows Grant Number 20J11318 (TY) and by JSPS KAKENHI Grant Numbers JP20K03831 (TK).

[1] K. Schwab, E. A. Henriksen, J. M. Worlock, and M. L. Roukes, *Nature* **404**, 974 (2000).

[2] M. Meschke, W. Guichard, and J. P. Pekola, *Nature* **444**, 187 (2006).

[3] A. V. Timofeev, M. Helle, M. Meschke, M. Möttönen, and J. P. Pekola, *Phys. Rev. Lett.* **102**, 200801 (2009).

[4] J. P. Pekola, *Nat. Phys.* **11**, 118 (2015).

[5] N. Li, J. Ren, L. Wang, G. Zhang, P. Hägggi, and B. Li, *Rev. Mod. Phys.* **84**, 1045 (2012).

[6] D. Segal and A. Nitzan, *Phys. Rev. Lett.* **94**, 034301 (2005).

[7] T. Ruokola, T. Ojanen, and A. P. Jauho, *Phys. Rev. B* **79**, 144306 (2009).

[8] T. Ojanen and A. P. Jauho, *Phys. Rev. Lett.* **100**, 155902 (2008).

[9] K. Joulain, J. Drevillon, Y. Ezzahri, and J. Ordonez-Miranda, *Phys. Rev. Lett.* **116**, 200601 (2016).

[10] M. Kilgour and D. Segal, *Phys. Rev. E* **98**, 012117 (2018).

[11] R. Uzdin, A. Levy, and R. Kosloff, *Phys. Rev. X* **5**, 031044 (2015).

[12] A. Ronzani, B. Karimi, J. Senior, Y.-C. Chang, J. T. Peltonen, C. Chen, and J. P. Pekola, *Nat. Phys.* **14**, 991 (2018).

[13] J. Senior, A. Gubaydullin, B. Karimi, J. T. Peltonen, J. Ankerhold, and J. P. Pekola, *Commun. Phys.* **3**, 40 (2020).

[14] J. Klatzow, J. N. Becker, P. M. Ledingham, C. Weinzel, K. T. Kaczmarek, D. J. Saunders, J. Nunn, I. A. Walsley, R. Uzdin, and E. Poem, *Phys. Rev. Lett.* **122**, 110601 (2019).

[15] Z. L. Xiang, S. Ashhab, J. Q. You, and F. Nori, *85*, 623 (2013).

[16] A. F. Kockum, A. Miranowicz, S. De Liberato, S. Savasta, and F. Nori, *Nat. Rev. Phys.* **1**, 19 (2019).

[17] P. Forn-Díaz, L. Lamata, E. Rico, J. Kono, and E. Solano, *Rev. Mod. Phys.* **91**, 025005 (2019).

[18] Y. Nakamura, Y. A. Pashkin, and J. S. Tsai, *Nature* **398**, 786 (1999).

[19] J. E. Mooij, T. P. Orlando, L. Levitov, L. Tian, C. H. van der Wal, and S. Lloyd, *Science* **285**, 1036 (1999).

[20] J. Koch, T. M. Yu, J. Gambetta, A. A. Houck, D. I. Schuster, J. Majer, A. Blais, M. H. Devoret, S. M. Girvin, and R. J. Schoelkopf, *Phys. Rev. A* **76**, 042319 (2007).

[21] B. Karimi, F. Brange, P. Samuelsson, and J. P. Pekola, *Nat. Commun.* **11**, 67 (2020).

[22] O. Maillet, D. Subero, J. T. Peltonen, D. S. Golubev, and J. P. Pekola, *Nat. Commun.* **11**, 4326 (2020).

[23] C. Yang, X. Wei, J. Sheng, and H. Wu, *Nat. Commun.* **11**, 4656 (2020).

[24] A. J. Leggett, S. Chakravarty, A. T. Dorsey, M. P. Fisher, A. Garg, and W. Zwerger, *Rev. Mod. Phys.* **59**, 1 (1987).

[25] U. Weiss, *Quantum Dissipative Systems*. (World Scientific, Singapore, 2012).

[26] T. Ruokola and T. Ojanen, *Phys. Rev. B* **83**, 045417 (2011).

[27] K. Saito and T. Kato, *Phys. Rev. Lett.* **111**, 214301 (2013).

[28] Y. Yang and C. Q. Wu, *Europhys. Lett.* **107**, 30003 (2014).

[29] E. Taylor and D. Segal, *Phys. Rev. Lett.* **114**, 220401 (2015).

[30] C. Wang, J. Ren, and J. Cao, *Phys. Rev. A* **95**, 023610 (2017).

[31] T. Yamamoto, M. Kato, T. Kato, and K. Saito, *New J. Phys.* **20**, 093014 (2018).

[32] T. Yamamoto and T. Kato, *Phys. Rev. B* **98**, 245412 (2018).

[33] D. Braak, *Phys. Rev. Lett.* **107**, 100401 (2011).

[34] In general, the two-state system includes a detuning energy, $-\hbar\omega\sigma_z$. In this paper, we consider the zero-detuning case ($\omega = 0$) for simplicity.

[35] A. Garg, J. N. Onuchic, and V. Ambegaokar, *J. Chem. Phys.* **83**, 4491 (1985).

[36] M. C. Goorden, M. Thorwart, and M. Grifoni, *Phys. Rev. Lett.* **93**, 267005 (2004).

[37] D. Zueco and J. García-Ripoll, *Phys. Rev. A* **99**, 013807 (2019).

[38] L. Magazzù and M. Grifoni, *J. Stat. Mech.* **2019**, 104002 (2019).

[39] Y. Meir and N. S. Wingreen, *Phys. Rev. Lett.* **68**, 2512 (1992).

[40] K. Saito, *Europhys. Lett.* **83**, 50006 (2008).

[41] D. Segal, A. J. Millis, and D. R. Reichman, *Phys. Rev. B* **82**, 205323 (2010).

[42] F. Nesi, M. Grifoni, and E. Paladino, *New J. Phys.* **9**, 316 (2007).

[43] Although the ratio between a_1 and a_2 is also relevant to the appearance of the two peaks, it is a minor effect.

[44] M. Thorwart, L. Hartmann, I. Goychuk, and P. Hägggi, *J. Mod. Opt.* **47**, 2905 (2000).

[45] S. J. Bosman, M. F. Gely, V. Singh, A. Bruno, D. Bothner, and G. A. Steele, *npj Quantum Inf.* **3**, 46 (2017).

[46] P. Forn-Díaz, J. Lisenfeld, D. Marcos, J. J. García-Ripoll, E. Solano, C. J. P. M. Harmans, and J. E. Mooij, *Phys. Rev. Lett.* **105**, 237001 (2010).

[47] P. Forn-Díaz, G. Romero, C. J. Harmans, E. Solano, and J. E. Mooij, *Sci. Rep.* **6**, 26720 (2016).

[48] T. Niemczyk, F. Deppe, H. Huebl, E. P. Menzel, F. Hocke, M. J. Schwarz, J. J. García-Ripoll, D. Zueco, T. Hümmer, E. Solano, A. Marx, and R. Gross, *Nat. Phys.* **6**, 772 (2010).